C.P. No. 59
12483
A.R.C. Technical Report

MINISTRY OF SUPPLY

AERONAUTICAL RESEARCH COUNCIL

CURRENT PAPERS

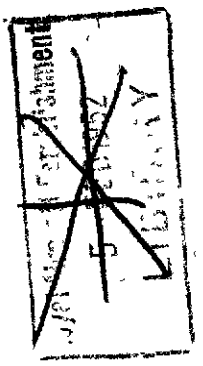

Measurement of Heat Transfer and Skin Friction at Supersonic Speeds

Preliminary Results of Measurements on Flat Plate at Mach Number of 2.5

By

J. E. Johnson and R. J. Monaghan

C.P. No.59

Technical Note No. Aero.1994
SD.91
April, 1949.

ROYAL AIRCRAFT ESTABLISHMENT

The Measurement of Heat Transfer and Skin Friction at Supersonic Speeds: Preliminary Results of Measurements on a Flat Plate at a Mach number of 2.5

by

J.E.Johnson
and
R.J.Monaghan

SUMMARY

This report gives details of a 5" × 5" supersonic tunnel designed for heat transfer and boundary layer research and the preliminary results obtained with it at a Mach number of 2.5. A steam heated copper plate 5" × 14" is let into one wall and provision is made for measuring the plate temperature T_p and the heat dissipated from the plate to the air stream over a range of temperature differences. Measurements of boundary layer profile and plate temperature without heat transfer have also been made.

The ratio of stagnation temperature to wall temperature for zero heat transfer (kinetic temperature) was found to be $\frac{T_o}{T_w} = 1.07$ giving $\frac{T_w - T_1}{T_o - T_1} = 0.88$ which compares with Squire's theoretical estimates of $\sigma^{1/3} = 0.896$ (turbulent boundary layers) and $\sigma^{1/2} = 0.849$ (laminar), for Prandtl No. $\sigma = 0.72$. Within the range tested, the heat transfer was proportional to the difference between the actual plate temperature T_p and the plate temperature giving zero heat transfer T_w and was also independent of the temperature level. The velocity profile of the boundary layer on the plate agreed well with the profile for incompressible turbulent flow. Calculation of mean heat transfer coefficients from the boundary layer measurements, using Von Karman's relation between skin friction and heat transfer, agreed with the heat transfer measurements within the limits of the scatter of the experiments.

LIST OF CONTENTS

		Page
1	Introduction	4
2	Description of Apparatus	4
3	Analysis of Test Results	6
4	Experimental Results	8
5	Correlation of Heat Transfer Results with Boundary Layer Measurements and with Theory	10
6	Conclusions	14
References		15

LIST OF TABLES

	Table
Shape of Nozzle	I
Heat Transfer Measurements	II
Measurements of Boundary Layer on Dummy Hot Plate in Zero Heat Transfer Condition	III

LIST OF ILLUSTRATIONS

	Figure
General Arrangement of Supersonic Heat Transfer Tunnel (Gas 7336)	1
Details of Steam Heated Plate (Gas 7337)	2
Diagram of Steam and Water Connections (Atmospheric Pressure) (Gas 7338)	3
Diagram of Steam and Water Connections (Reduced Pressure) (Gas 7339)	4
Location of Static Pressure Points in Tunnel and Hot Plate (Gas 7340)	5
Arrangement of Manometers (Gas 7341)	6
Diagram of Compensator Circuit (Gas 7342)	7
Variation of Heat Transfer with Temperature Ratio (Gas 7343)	8
Variation of Heat Transfer with Temperature Ratio (faired) (Gas 7344)	9

LIST OF ILLUSTRATIONS (CONTD.) Figure

Velocity Profiles on Boundary Layer in Zero Heat Transfer Condition (Gas 7349) 14

Upper and Lower Limits to Free Stream Mach Number Distribution Along Tunnel (Gas 7350) 15

Ratio of Displacement Thickness to Momentum Thickness (Zero Heat Transfer Conditions) (Gas 7351) 16

Boundary Layer Thickness in the Zero Heat Transfer Condition (Gas 7352) 17

1 Introduction

Experimental confirmation was required of theoretical predictions of the heat transfer coefficients and kinetic temperatures obtained on bodies immersed in supersonic air streams. The tunnel to be described in this report was built to suit the R.A.E. Altitude Test Plant and a Mach number of 2.5 was chosen as being the highest obtainable with a reasonable size of tunnel. It was realised that for obtaining known boundary layer conditions on the heat transfer surface it should be in the form of a streamlined body located in the centre of the air stream free from the effects of the boundary layer on the walls. A preliminary design for such a body was prepared but considerable difficulties in obtaining uniform heating and accurately measuring the heat dissipation from such a body were encountered. It was therefore decided, in the first instance, to make measurements from a heated surface let into one wall of the tunnel and to try to obtain similar boundary layer conditions to those on a central body by providing a slot at the leading edge of the surface through which the boundary layer could be removed by suction.

Preliminary checks of the tunnel performance were made with a dummy wooden plate in place of the heated copper plate. The results showed that it was necessary to taper the nozzle walls outwards towards the exit to obtain an approximately constant Mach number in the working section. The average Mach number then obtained was close to 2.5. A traverse through the boundary layer near the leading edge of the plate with a pitot tube 0.018" dia. indicated that with no suction on the slot the boundary layer was about 0.2" thick. Owing to the low pressure in the tunnel the largest vacuum pump then available could only remove a small quantity of air through the slot and this had no appreciable effect on the boundary layer even when the plate was raised above the tunnel wall and a leading instead of a trailing entry provided for the suction slot. Steps have been taken to provide a larger suction capacity and in the meantime the hot plate was installed and some measurements of heat transfer were made with the plate level with the walls and without any suction on the slot in order to gain experience on the technique of heat transfer measurement in the tunnel. This report contains a description of the tunnel, hot plate and experimental apparatus used and gives details of the results obtained in the above conditions. When the larger suction capacity is available further efforts will be made to remove the boundary layer completely from the leading edge and so obtain a laminar boundary layer starting at the leading edge of the plate and persisting as far back as possible.

2 Description of Apparatus

The general arrangement of the tunnel as set up for heat transfer measurements is shown on Fig.1. The tunnel is operated with its axis horizontal and the hot plate vertical. Dry air is supplied to the tunnel at atmospheric pressure from a refrigerating and heating plant, the temperature of the air can be varied between -50°C and +60°C. The air is exhausted from the tunnel by the Altitude Test Plant.

2.1 Nozzle Design

The nozzle shape was determined graphically using Busemann's method, no allowance being made for boundary layer. Table I gives details of the shape used. The leading dimensions were originally

Entrance	5 × 6.5 inches
Throat	5 × 1.808 inches
Working section	5 × 5 inches
Length of nozzle	15.8 inches
Length of duct	20.2 inches
Length of test plate including guard ring	14.0 inches

When the width of the tunnel at the exit end was increased to allow for the boundary layer the dimensions became

Entrance	5 × 6.46 inches
Throat	5 × 1.808 inches
Exit section	5 × 5.236 inches

The designed operating conditions for the nozzle are

Pressure ratio P/P_o = 0.055

Mach number $M = u/a$ = 2.548

Temperature ratio T_1/T_o = 0.436

where P = pressure at end of nozzle.

P_o = stagnation pressure.

u = velocity at end of nozzle.

a = velocity of sound in air at the conditions at end of nozzle.

T_1 = free stream temperature (absolute) at end of nozzle.

T_o = stagnation temperature (absolute).

In practice the pressure ratios measured from the static holes in the hot plate had a mean value of 0.059 giving a mach number of 2.5.

2.2 Hot plate

The best method of supplying an accurately known quantity of heat to a body is by electricity. This method was considered when designing the hot plate but was abandoned because of the difficulty of ensuring a uniform plate temperature when the local rate of heat transfer is expected to vary considerably over the area. An indirect electrical method was therefore chosen in which the plate is heated by steam, the required quantity of steam being generated in an electrically heated boiler. By this means it can be ensured that the temperature of the plate remains practically constant in spite of large variations in the local rate of heat flow.

The general arrangement of the hot plate is shown on Fig.2 and the diagrammatic arrangement of the steam heating circuit is shown on Fig.3. The hot plate and its associated guard ring were milled out from a solid block of copper. The guard ring surrounds the plate on all four edges, separated from it by an air gap except for a thin connecting link of copper to preserve a smooth surface. The interior of the plate is well ribbed for stiffness and to promote a high rate of heat transfer between steam and plate. Heat flow from the back of the plate is minimised by a thick copper plate attached to the guard ring and separated from the hot plate by a small air gap. To prevent the accumulation of air in the steam space, the electric boiler

is adjusted to supply more steam than required by the plate and the surplus is taken out from the bottom of the plate and condensed in a small cooler. Any entrained air is carried out by the surplus steam. The electrical input to the boiler is measured and the condensate is collected over a known time and weighed. From this the heat dissipated from the plate can be calculated allowing for all losses. The boiler and connecting pipes are carefully insulated. The guard ring is maintained at the same temperature as the plate by circulation of steam from an independent supply at the same pressure as in the boiler. In order to demonstrate that the heat transfer is proportional to temperature difference and to provide a check on the plate temperature required for zero heat transfer, a number of tests were run at a reduced steam pressure. For this purpose the steam circuit is as shown in Fig.4. The circuit is coupled to the main vacuum pump line which gives a steam temperature of about 55°C. It is then possible to obtain a stagnation temperature slightly in excess of the plate temperature.

2.3 Pressure measurements

Fig.5 shows the points at which provision is made for measuring the static pressure both in the tunnel walls and in the hot plate. Fig.6 shows diagrammatically the connections between the manometers and the tunnel. It was found necessary to fit by-passes round several of the water manometers to prevent the level rising too high during starting. Each bank of water manometers is connected to a mercury reference manometer. A special mercury sloping gauge was constructed to read directly absolute pressures up to about 3" Hg. with a three-way connection to each bank of water manometers. The diameter of the pressure measuring holes in the tunnel walls and the hot plate is about 1/32 inch.

2.4 Temperature measurements

Fig.2 shows that provision is made for fitting thermocouples into the hot plate between each pressure measuring point along the centre line. The thermocouple wires are of manganin and constantan 0.2 mm. diameter silk and enamel covered. The junction is made in the plate by driving a copper peg into a small hole in the plate through which the bared ends of the wire protrude. The face of the plate is afterwards filed flush and polished. The junctions are connected through a double-pole 15-way switch to a compensator, the circuit of which is shown diagrammatically in Fig.7. It will be seen that the e.m.f. of the couple is balanced by a sensitive mirror galvanometer against voltage drop across a resistance of known value. The current required to balance the e.m.f. of the couple is then a measure of the couple e.m.f. and hence the temperature of the hot junction and is read on a sensitive amp. meter. The cold junction is maintained at 0°C in a flask of ice and water.

The shunt on the meter is adjusted so that 100 divisions on the scale correspond approximately to a temperature difference of 100°C. There are 12 couples on the plate, the remaining positions on the switch are used for measuring room temperature, stagnation temperature at the tunnel entrance and air temperature at the nozzle in the boundary layer

3.1 Stagnation pressure and temperature

As the air is not drawn in to the tunnel directly from the atmosphere but comes from the drying and heating plant through a long pipe it is necessary to calculate the true stagnation pressure and temperature. The stagnation pressure can be obtained from the static pressure at the entrance to the tunnel when the areas of the entrance and throat are known and assuming isentropic flow between the two. In this way it was found that

$$P_o = 1.021\ P$$

where P is the static pressure at the entrance and P_o is the stagnation pressure.

The maximum velocity of the air at the tunnel entrance is of the order of 180 ft./sec. so that the difference between the stagnation temperature and the temperature measured by the thermocouple in the air stream is of the order of $0.2^{\circ}C$. The mercury thermometer is however located in the large duct in front of the tunnel where the velocity is much lower so that the correction is negligible.

3.2 Wall temperature

In order to determine the heat transfer coefficient from heat flow measurements it is necessary to define the temperature difference giving rise to the heat flow. In this case the upper temperature is easily determined from the readings of the thermocouples embedded in the surface of the hot plate. The lower temperature, that is, the effective air temperature, is not so easily arrived at. The free stream temperature T is obviously not the appropriate one to use as air at free stream velocity can never be directly in contact with the stationary plate surface owing to the boundary layer. It can also be shown that owing to the exchange of heat in the boundary layer the stationary layer of air in contact with the wall when no heat is flowing through the wall does not quite attain stagnation temperature T_o but is slightly lower. This wall temperature at zero heat flow, sometimes called the kinetic temperature may be defined by the equation

$$T_w = T + \frac{\beta u^2}{2gJc_p}$$

Similarly

$$T_o = T + \frac{u^2}{2gJc_p}$$

$$\therefore\ T_o - T_w = \frac{u^2}{2gJc_p}(1 - \beta) = \Delta t$$

which may be reduced to

$$\Delta t = T_o \left[1 - \left(\frac{P}{P_o}\right)^{\frac{\gamma-1}{\gamma}}\right](1 - \beta)$$

Several determinations of β were made after the conclusion of the heat transfer tests and are described in detail in para. 4.1.

3.3 Heat losses from hot plate and boiler

The net heat dissipation from the hot plate to the air stream is obtained by subtracting various losses from the total electrical input

to the boiler. The sources of heat loss are:- surplus steam from the hot plate, heat loss from boiler, connecting pipes and manometer, heat loss to the adjacent tunnel wall by conduction, and heat loss from the hot plate surface to the inside of the tunnel by radiation.

The heat lost from the surplus steam is readily calculated from the amount of condensate collected during an experiment. The heat lost by conduction from boiler manometers etc. and from the hot plate to the tunnel is calculated from the results of a test where heat loss from the surface of the plate was prevented by an insulating layer of cork. The loss by radiation from the plate is calculated assuming average emissivities for copper and tunnel surfaces.

4 Experimental Results

The programme of tests was arranged to give measurements of heat transfer over as wide a range of temperature as possible in order to verify that heat transfer is proportional to the temperature difference between the kinetic temperature in the boundary layer and the temperature of the hot plate. The lowest stagnation temperature obtained was -50°C and the highest +62°C. As mentioned in para.2.2 a number of tests were done with the steam circuit connected to the vacuum pumps to reduce the hot plate temperature from 100°C to about 55°C, giving values of $T_p - T_w$ quite close to zero.

The results of the heat transfer measurements are given in detail in Table II. In Fig.8 they are plotted in the form of $\frac{Q6}{A_1 T_p}$ against $\frac{T_o}{T_p}$ to show the relationship between heat transfer and temperature difference. It will be seen that there is a certain amount of scatter in the results and that they are not quite on a straight line. In Fig.9 the same results are plotted after having been corrected for variation in air flow due to change of barometric pressure and after fairing onto a constant value of $\frac{u_1}{\nu_1} = 2.54 \times 10^5 \left(\frac{1}{\text{inches}}\right) \left[\text{or } 10^7 \frac{1}{\text{metres}}\right]$, where

u_1 = free stream velocity

ν_1 = kinematic viscosity at free stream conditions.

The points now lie quite close to a straight line which meets the abscissa at a value of $\frac{T_o}{T_p} = 1.07$. As will be shown later this value agrees closely with that measured without heat transfer. From this evidence a mean heat transfer coefficient $\overline{K}_H$ can be derived from the experimental results by the formula

$$\overline{K}_H = \frac{Q6}{A_1 \rho_1 u_1 c_p g (T_p - T_w)}$$

Values of $\bar{k}_H$ are plotted against $\frac{u_1}{\nu_1}$ on Fig.10.

4.1 Measurement of kinetic temperature

Owing to the exchange of heat between the low speed regions of the boundary layer and the free stream air, the wall of the tunnel does not quite attain stagnation temperature when no heat flows through the walls. As already explained, it is necessary to know this temperature to obtain the effective temperature difference for heat transfer. In order to measure the kinetic temperature it is necessary to be quite sure that no heat is being transferred through the walls. This condition was obtained by raising the stagnation temperature in the tunnel above room temperature until the kinetic temperature was equal to the room temperature. Fig.11 shows the experimental rig used to ensure that the correct conditions were being obtained. The copper plate as used for the heat tests was fitted in the tunnel, but instead of the boiler a vacuum pump was coupled up so that air from the room was drawn through both the guard ring and the plate. Thermometers were fitted in the inlet and outlet pipes and gave quite a sensitive indication of whether any heat was being transferred to or from the plate.

The test procedure was to operate the tunnel for a short time at a stagnation temperature a little below the value necessary for zero heat transfer and to heat up the tunnel air supply gradually until the zero point was passed, recording at frequent intervals the stagnation temperature, plate temperature, inlet and outlet circulating air temperatures and room temperature. The process was then repeated with the stagnation temperature slowly falling. It was found that there was an appreciable time lag between the change of stagnation temperature and change of temperature difference in the circulating air due to the heat capacity of the copper plate and some difficulty was experienced in controlling the tunnel air heaters to give sufficiently slow and smooth changes of temperature. Fig.12 shows a typical time and temperature chart for one of these experiments. From these it is quite easy to pick out the conditions required for zero heat transfer.

The following table gives the results obtained from several observations, taken with increasing and decreasing stagnation temperatures. The value of $\frac{T_o}{T_p}$ is about 1% lower for decreasing stagnation temperatures than for increasing temperatures. The average value of 1.071 agrees very close with the intersection of the line through the heat transfer results on Fig.9.

Test No.	Wall Temperature T_w °C abs.	Stagnation Temperature T_o °C abs	$\frac{T_o}{T_w}$	$\beta = \frac{\frac{T_w}{T_o} - \frac{T_1}{T_o}}{1 - \frac{T_1}{T_o}}$	Direction of change of stagnation temperature T_o
40	294.7	318.0	1.079	0.8683	ascending
40	296.0	318.9	1.077	0.8713	ascending
41	287.9	309.1	1.074	0.8760	ascending
40	295.4	315.0	1.068	0.8853	descending
41	287.4	305.0	1.061	0.8965	descending
41	288.1	307.7	1.068	0.8853	descending
Mean	-	-	1.071	0.8805	-

4.2 Measurements of boundary layer

In order to correlate the heat transfer results with theoretical estimates it is necessary to have measurements of the boundary layer on the plate. For this purpose a wooden model of the hot plate was made and fitted into the tunnel; new side walls were also made incorporating observation windows. A number of holes were drilled in the tunnel wall opposite to the plate into which a pitot tube was fitted. The pitot tube was fitted with a micrometer traversing gear enabling the distance of the tube from the wall to be measured to 1/1000 inch. The measuring tube was made from hypodermic needle 0.018 inch diameter. Full details of the tube and traversing gear are given on Figs.5 and 6 of Ref.2. By this means the velocity distribution in the boundary layer without heat transfer was measured at various distances from the leading edge of the plate.

5 Correlation of Experimental Heat Transfer Results with Boundary Layer Measurements and with Theory

5.1 Mean heat transfer coefficient $\bar{k}_H$ and its experimental variation with $\frac{T_o}{T_p}$ and $\left(\frac{u_1}{\nu_1}\right)$

Measurements of the plate temperature in the zero heat transfer condition have shown that

$$1.06 \leqslant \frac{T_o}{T_p} \leqslant 1.08$$

Also extrapolation of plots of the rate of heat transfer from the plate against $\frac{T_o}{T_p}$ has shown that the heat flow becomes zero when

$$\frac{T_o}{T_p} = 1.07 \quad \text{for Mach Number } M = 2.5.$$

This corresponds to

$$\frac{T_w - T_1}{T_o - T_1} = 0.88 = \sigma^{0.4} \quad \text{for } \sigma = 0.72,$$

where T_w = adiabatic wall temperature (kinetic temperature)

T_1 = free stream temperature

T_o = stagnation temperature

σ = Prandtl number $\left(\frac{c_p \mu}{k}\right)$

The value $\sigma^{1/3}$ (=0.896) has been quoted by Squire[1] for turbulent boundary layers in low speed flow.

The variation of $\bar{k}_H$ with $\frac{u_1}{\nu_1}$ is shown on Fig.10. The broken lines show a variation as $\left(\frac{u_1}{\nu_1}\right)^{-1/5}$ which fits reasonably well despite

the scatter of the experimental results. This is the variation which is satisfied approximately by turbulent boundary layers in low speed flows for Reynolds numbers greater than 10^6.

As the boundary layer has only been measured for the zero heat transfer case it is necessary to show that heat transfer coefficients calculated for this case are of general validity. Fig.13 shows that this is the case within the limits of the range of $\frac{T_o}{T_p}$ covered by the tests. In this figure the experimental values of k_H have been brought to $\frac{u_1}{\nu_1} = 2.54 \times 10^5 \left(\frac{1}{\text{inches}}\right) \left[= 10^7 \frac{1}{\text{metres}}\right]$ assuming a 1/5th power variation and plotted against $\frac{T_o}{T_p}$. The results show a scatter of about $\pm 5\%$ about a mean but there is no sign of any consistent variation with temperature.

5.2 Boundary layer conditions

Fig.14 shows the velocity profile measured at different distances from the leading edge of the plate (from 1.3 to 10.3 inches). For the condition of zero heat transfer with the dummy plate on which these measurements were made, $\frac{u_1}{\nu_1} = 2.4 \times 10^5 \left(\frac{1}{\text{inches}}\right)$. The variation of free stream Mach number along the tunnel as deduced from the static pressure measurements along the plate and along the opposite wall are shown on Fig.15. The Reynolds number values are based on distance from the effective starting point of the boundary layer as determined later. The values of u/u_1 were determined from the pitot measurements using Rayleigh's pitot tube formula and assuming constant* total energy across the boundary layer. Values of the displacement thickness δ^* were computed from the formula

$$\delta^* = \int_0^s \left(1 - \frac{\rho u}{\rho_1 u_1}\right) dy$$

where u is the velocity at the point of measurement in the boundary layer

ρ is the density at the point of measurement

u_1 is the free stream velocity

ρ_1 is the free stream density

y is the distance from the wall to the centre of the pitot orifice

δ is the full boundary layer thickness.

The displacement thickness is used in preference to the full boundary layer thickness because of the indefinite nature of the latter.

All the profiles shown are of a fully turbulent nature. For small values of y/δ* they follow the 1/7th power law of Blasius*, but for larger values the variation is closer to a 1/6th power law. The best agreement over the whole range is obtained with the broken line derived by Schultz-Grunow[3] from low speed tests at $R_{e_x} = 10^7$. This indicates that compressibility has little effect on the zero heat transfer turbulent velocity profile, except possibly very close to the wall where the experimental results are in any case less accurate.

The experimental ratios of displacement thickness to momentum thickness are shown on Fig.16 and Table III and compared with values calculated from 1/5, 1/7 and 1/9th power laws. The momentum thickness θ was calculated by the formula

$$\theta = \int_0^{\delta} \frac{\rho u}{\rho_1 u_1} \left(1 - \frac{u}{u_1}\right) dy \qquad (1)$$

The free stream Mach number is taken as that measured at the outer edge of the boundary layer by the pitot in conjunction with the static pressure at the wall. Here again the experimental values lie between the 1/6th and 1/7th power law variations.

The use of a 1/7th power law as a working approximation therefore seems justified, particularly as it is in agreement with low speed results of about the same Reynolds number.

If

$$\frac{u}{u_1} = (y/\delta)^{1/7}$$

then

$$\delta = k R_{e_x}^{-1/5} x \qquad (2)$$

where x is the distance from the start of the boundary layer, and k is a constant. Therefore $\delta^{5/4} \left(\frac{u_1}{\nu_1}\right)^{1/4}$ should be a linear function of x. Values of this are plotted on Fig.17 against the distance x from the leading edge of the plate. The values taken for δ are the means between the values obtained by scaling up the momentum and displacement thickness according to the 1/7th power law from Table III.

Three series of measurements of the boundary layer on the dummy hot plate were made. The first series (symbol "x") were made before the

* This states that

heat transfer tests and were not sufficient in number to determine the profile properly. The second series (symbol "⊙") were made when the dummy plate was replaced at the conclusion of the heat tests and gave results greater than the original series except for the position in front of the leading edge of the plate, indicating a disturbance at the leading edge producing thickening of the boundary layer on the plate. This was attributed to air leaking into the tunnel through the suction slot and a third series of measurements (symbol "+") was made with a small amount of suction applied to neutralize the leakage. These results agree well with the original series enabling a mean curve to be drawn such that

$$\delta = 0.418\ R_{e_x}^{-1/5}\ X \qquad (3)$$

where

$$X = x + 7.5$$

indicating an effective start for the boundary layer 7.5 inches ahead of the leading edge of the plate. A similar curve through the second series of measurements without suction gives

$$\delta = 0.461\ R_{e_x}^{-1/5}\ X \qquad (4)$$

where

$$X = x + 7.8$$

As it was not possible to be certain that there were no leaks during the heat transfer tests, especially as sealing was more difficult with the hot plate, it was decided to evaluate skin friction and heat transfer coefficients using both boundary layer profiles. Equation (3) will be called "Boundary Layer Approximation No.1" and equation (4) will be "Boundary Layer Approximation No.2".

5.3 Calculation of mean heat transfer coefficients from the experimental boundary layer profiles

For a flat plate in an air stream without pressure gradients, the momentum equation gives

$$\frac{\tau_o}{\rho_1 u_1^2} = \frac{\partial \theta}{\partial x} \qquad (5)$$

where τ_o is the local shearing stress at the plate (skin friction) and θ is the momentum thickness.

$\left(\frac{\theta}{\delta}\right)$ is given by equation (1) and for $\frac{u}{u_1} = (y/\delta)^{1/7}$, constant total energy and M = 2.5

$$\frac{\theta}{\delta} = 0.0695$$

Using either equation (3) or (4) and substituting for δ, expressions for $\frac{\tau_o}{\rho_1 u_1^2}$ can be obtained, in the zero heat transfer case, in terms of $\left(\frac{u_1}{\nu_1}\right)$ $\left[= 2.4 \times 10^5\right]$ and X.

Assuming that Von Karmans extension of Reynolds analogy between turbulent heat transfer and skin friction is valid and using the constants given in Ref.4 and a Prandtl number $\sigma = 0.72$, then

$$\frac{1}{k_H} = \frac{\rho_1 u_1^2}{\tau_o} - 2.68\sqrt{\frac{\rho_1 u_1^2}{\tau_o}}$$

from which k_H can be determined as a function of X. Integrating between values of X corresponding to the leading and trailing edges of the plate and dividing the result by plate length gives values of the mean heat transfer coefficient $\bar{k}_H$. The values of $\bar{k}_H$ calculated by this method from the two boundary layer approximations of para. 5.2 are shown on Figs.10 and 13. It will be seen that the majority of the experimental results lie between these two values.

It is possible that the scatter of the heat transfer results was due to variations in boundary layer thickness caused by leakage round the plate. There is also some indication of a thickening of the boundary layer caused by the slot without leakage so that a completely undisturbed boundary layer might give a result slightly lower than that given by approximation number 1.

6 Conclusions

The design of the hot plate and the method of measuring heat transfer appear to be quite satisfactory provided that leaks are kept to a minimum. The present results show a scatter of about $\pm 5\%$ but it is thought that this could be reduced with greater attention to reduction of leaks. The velocity distribution in the tunnel is adequate for the purpose of these tests and a reasonably constant Mach number is obtained. The slot for removal of the boundary layer by suction was not effective and requires to be made much larger and to have a leading instead of a trailing entry.

Direct measurement of wall temperature for zero heat transfer (kinetic temperature) and extrapolation of the heat transfer tests are in close agreement in giving a value of $\frac{T_o}{T_w} = 1.07$ at a Mach number of 2.5 which leads to a value of $\beta = \frac{T_w - T_1}{T_o - T_1} = 0.88$ and compares with Squires'[1] estimate of $\sigma^{1/3} = 0.896$ for turbulent boundary layers and $\sigma^{1/2} = 0.849$ (laminar).

The experimental results show clearly that the heat transfer is proportional to difference between plate temperature and wall or kinetic temperature and that the heat transfer coefficient does not vary with $\frac{T_o}{T_p}$ within the range of temperatures covered by the tests, $(0.6 < \frac{T_o}{T_p} < 1.03)$.

edge of the plate and there is a discontinuity in the rate of growth of boundary layer at the leading edge of the plate. There is some doubt as to the actual boundary layer thickness during the heat tests but it is thought to lie between values given by the two relations

$$\delta = 0.418\, R_{e_x}^{-1/5} X \quad \text{where } X = x + 7.5 \text{ inches}$$

and

$$\delta = 0.461\, R_{e_x}^{-1/5} X \quad \text{where } X = x + 7.8 \text{ inches}$$

Calculation of average heat transfer coefficients $\bar{k}_H$ from these two estimates of boundary layer thickness assuming constant total energy in the boundary layer and using Von Karman's extension of Reynolds analogy gives upper and lower values which embrace the majority of the experimental points (Fig.10). From this it may be concluded that Von Karman's analogy is valid for compressible turbulent flow and that variation of the leakage round the plate would account for the scatter of the experimental results. The value of the results is limited by this variation and further tests should be made with better known and more constant boundary layer conditions on the plate.

No attempt can therefore be made at this stage of the work to compare the experimental results with theoretical estimates, except to state that a theory which gives higher results than those measured cannot be accepted whereas a lower result may be acceptable.

References

No.	Author	Title, etc.
1	Squire, H.B.	Heat Transfer Calculation for Aerofoils. R.& M. 1986. November 1942.
2	Lukasiewicz,J. and Royle,J.K.	Boundary Layer and Wake Investigation in Supersonic Flow. R.& M. 2613 - October, 1948.
3	Wieghardt,K.	Turbulent Boundary Layers. A.V.A. Monograph No.B.5. T.I.B. GDC/3224T. April 1948.
4	Edited by Goldstein	Modern Developments in Fluid Dynamics. Clarendon Press Oxford, 1938.

Wt.2078.CP.58.K3. Printed in Great Britain.

Table I

Shape of Nozzle

Distance from Throat x inches	Width of Nozzle y inches	Distance from Throat x inches	Width of Nozzle y inches
0.00	1.808	5.00	4.344
.25	.845	.25	.421
.50	.951	.50	.492
.75	2.132	.75	.558
1.00	.310	6.00	.620
.25	.483	.25	.676
.50	.651	.50	.727
.75	.814	.75	.774
2.00	.971	7.00	.816
.25	3.122	.25	.852
.50	.265	.50	.884
.75	.402	.75	.911
3.00	.532	8.00	.934
.25	.654	.25	.953
.50	.770	.50	.968
.75	.880	.75	.980
4.00	.985	9.00	.989
.25	4.083	.25	.996
.50	.175	.50	.999
.75	.262	.75	5.000

Table II

Heat Transfer Measurements

Expt. No.	Stagnation Temp. T_o °K.	Plate Temp. T_p °K.	$\frac{T_o}{T_p}$	Heat Flow $Q_6 \times 10^2$ k.cal./sec.	Heat Transfer $Q_6/A_1T_p \times 10^3$	Mass Velocity $\rho_1 u_1$ kg.sec./m^3	Heat Transfe Coeffic $\bar{k}_H \times$
24	243	371.6	0.654	15.5	11.2	9.59	1.27
24	243	371.5	0.654	15.5	11.2	9.59	1.27
25	225	371.9	0.606	17.8	12.8	10.19	1.23
25	225	371.9	0.606	17.5	12.6	10.18	1.21
27	223	371.9	0.599	17.5	12.6	10.16	1.19
27	222	372.0	0.598	17.3	12.8	10.16	1.18
28	272	371.9	0.732	12.0	8.66	9.10	1.28
28	272	371.9	0.732	11.9	8.55	9.08	1.26
29	285	371.9	0.768	10.7	7.71	8.87	1.30
29	286	372.0	0.769	10.6	7.64	8.86	1.30
43	315	324.6	0.971	3.10	2.56	8.52	1.38
44	328	324.8	1.010	1.77	1.46	8.34	1.34
44	327	324.7	1.006	1.85	1.53	8.34	1.30
45	334	324.9	1.027	1.27	1.05	8.26	1.35
45	335	325.0	1.030	1.13	0.934	8.24	1.31
46	273	325.5	0.839	7.46	6.25	8.95	1.35
46	274	325.4	0.841	7.51	6.19	9.06	1.35
47	283	325.2	0.870	6.15	5.08	8.92	1.29
47	283	325.5	0.870	6.21	5.12	8.90	1.30
48	293	325.0	0.902	5.38	4.44	8.77	1.37
48	293	324.9	0.903	5.44	4.49	8.77	1.39
49	304	325.7	0.934	4.45	3.66	8.61	1.43

Table III

Measurements of boundary layer on du
not plate in zero heat transfer condi

x = distance downstream from leading edge

Description of Tests		x inches	M_1	$\frac{u_1}{\nu_1}$	δ^* inches
Early Tests No Suction	x	1.28	2.446	2.41×10^5	0.0563
		1.35	2.362	2.47×10^5	0.0587
		4.29	2.456	2.65×10^5	0.0761
		5.33	2.422	2.42×10^5	0.0780
		10.33	2.414	2.42×10^5	0.0949
Later Tests No Suction	⊙	1.26	2.448	2.29×10^5	0.0636
		5.35	2.460	2.28×10^5	0.0872
		10.35	2.416	2.36×10^5	0.1095
Later Tests With Suction	+	1.26	2.417	2.29×10^5	0.0587
		10.35	2.426	2.28×10^5	0.1034
Ahead of Plate	⊕	-0.9	2.381	2.44×10^5	0.0380

(δ is obtained from δ^* and θ by scaling up in accordar
power law velocity profile).

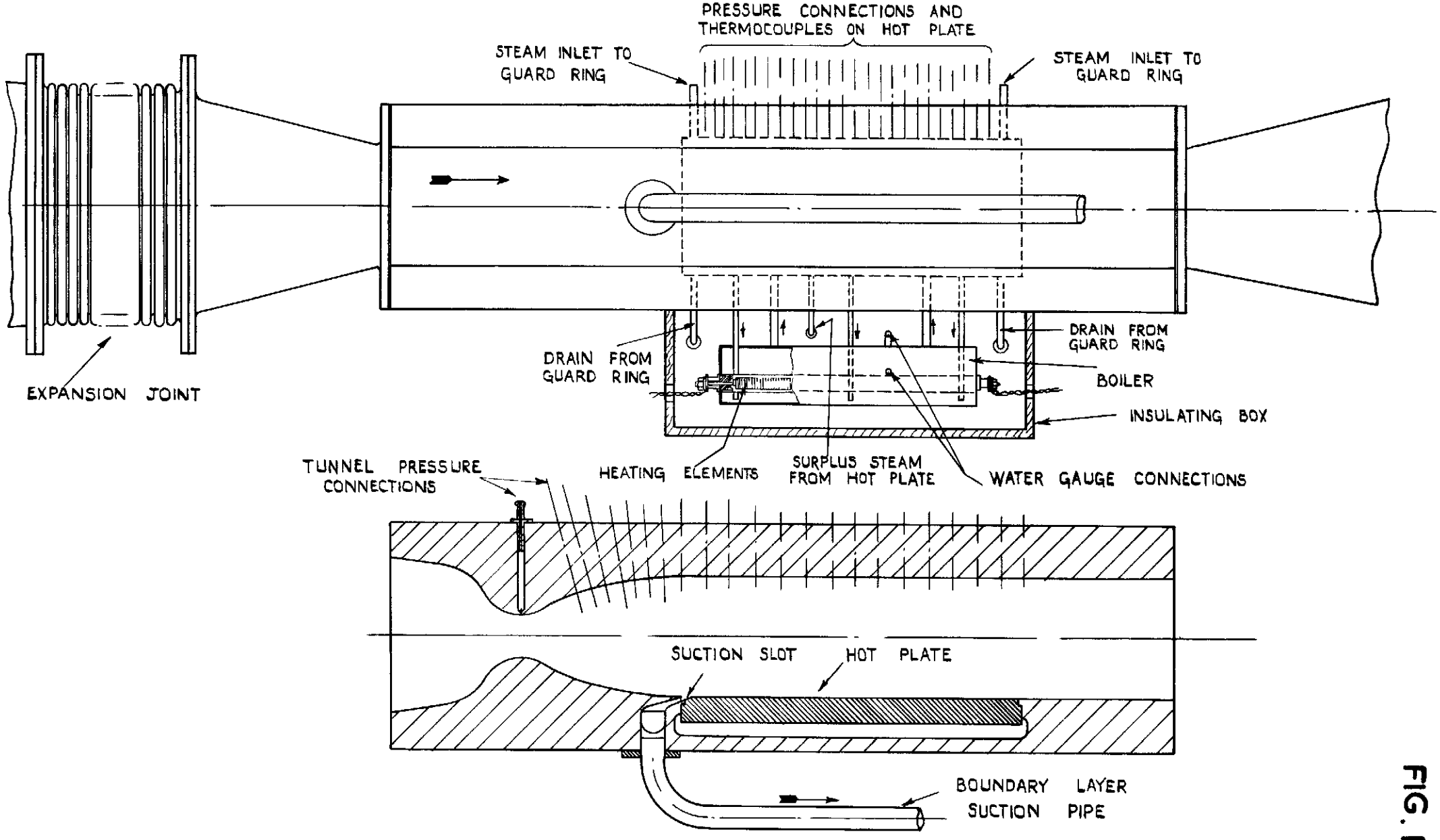

FIG.1. GENERAL ARRANGEMENT OF SUPERSONIC HEAT TRANSFER TUNNEL.

FIG. 1.

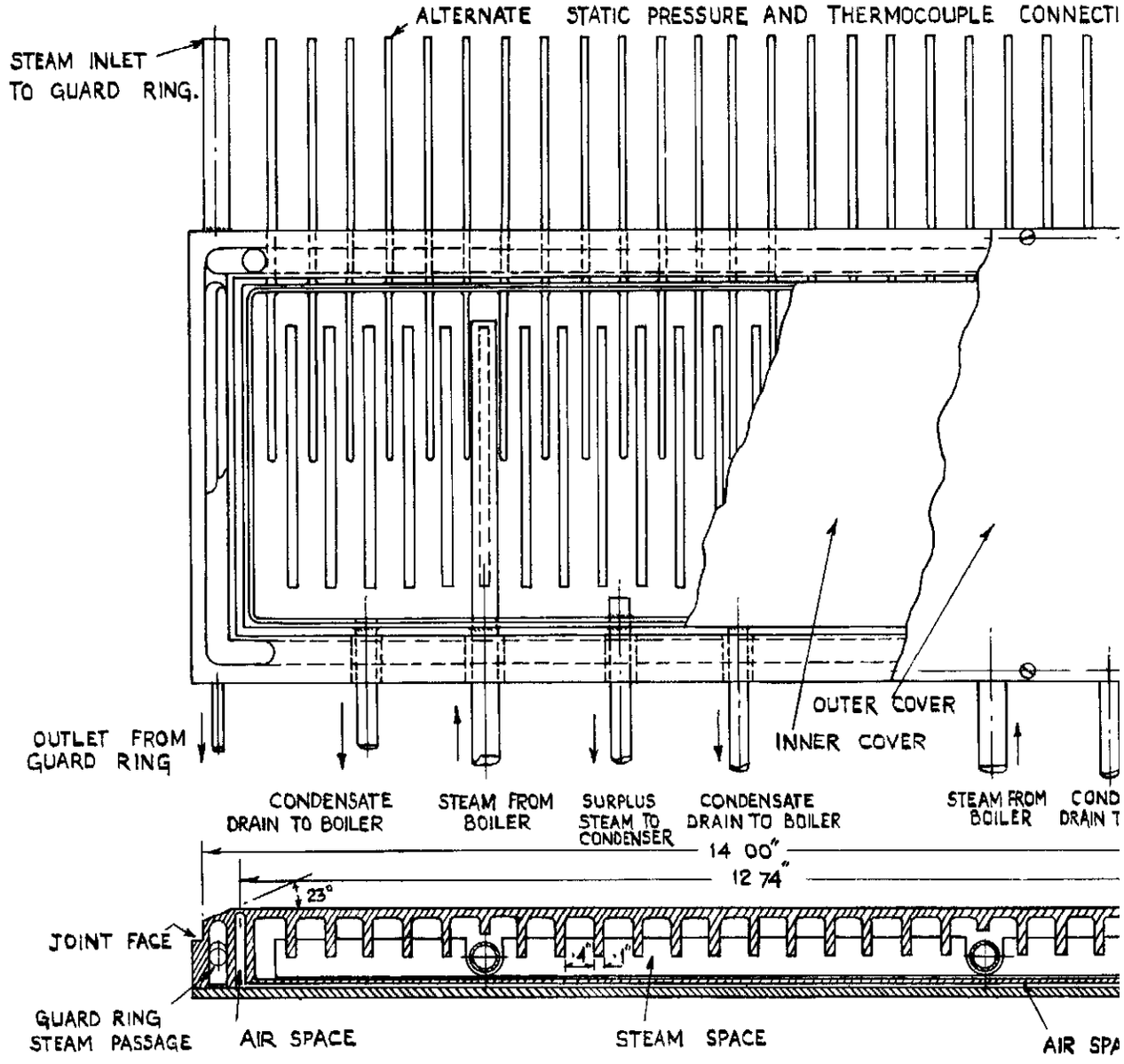

FIG. 2. DETAILS OF STEAM HEATED

FIG. 3.

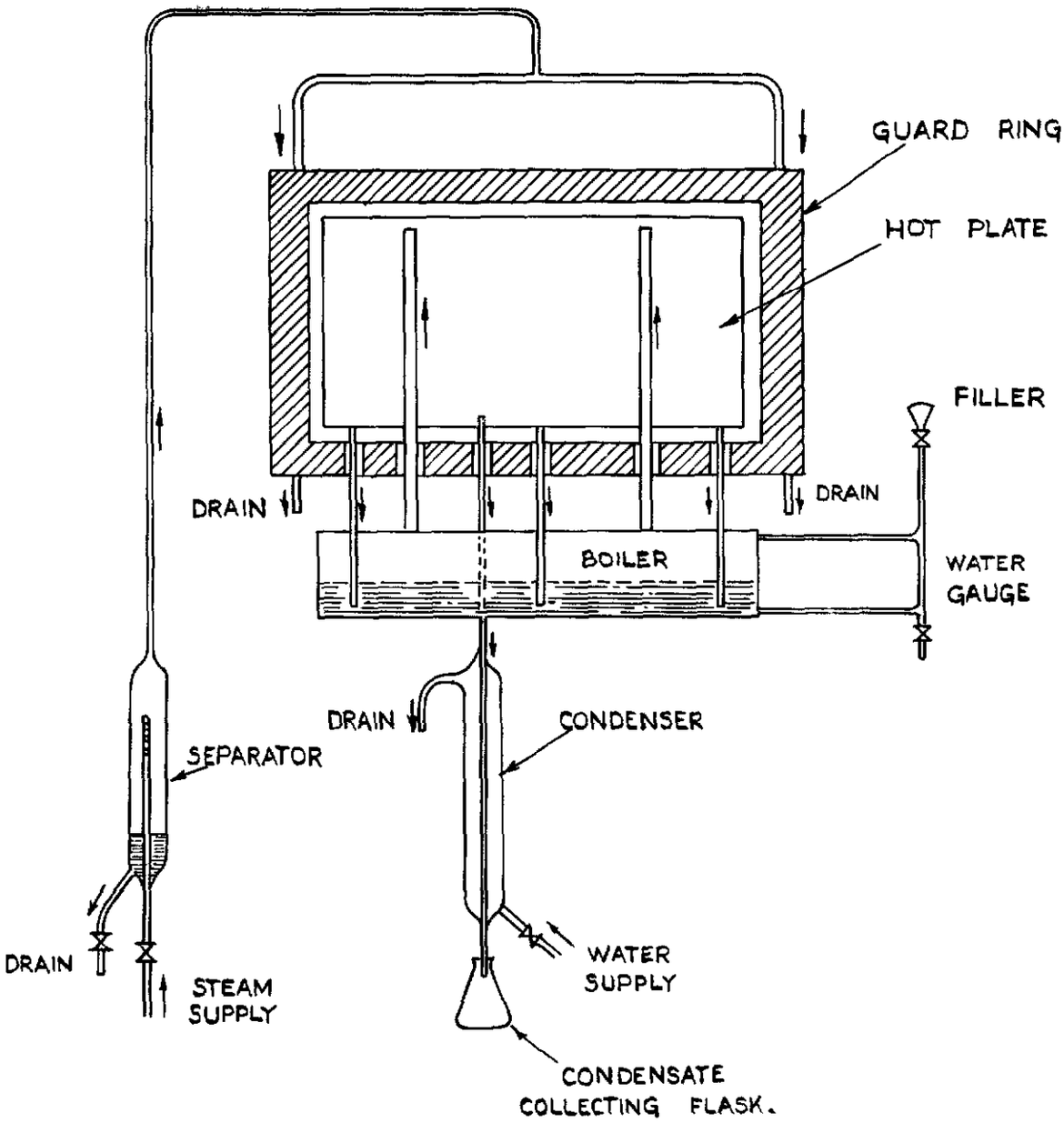

FIG. 3. DIAGRAM OF STEAM & WATER CONNECTIONS.
(ATMOSPHERIC PRESSURE)

FIG. 4.

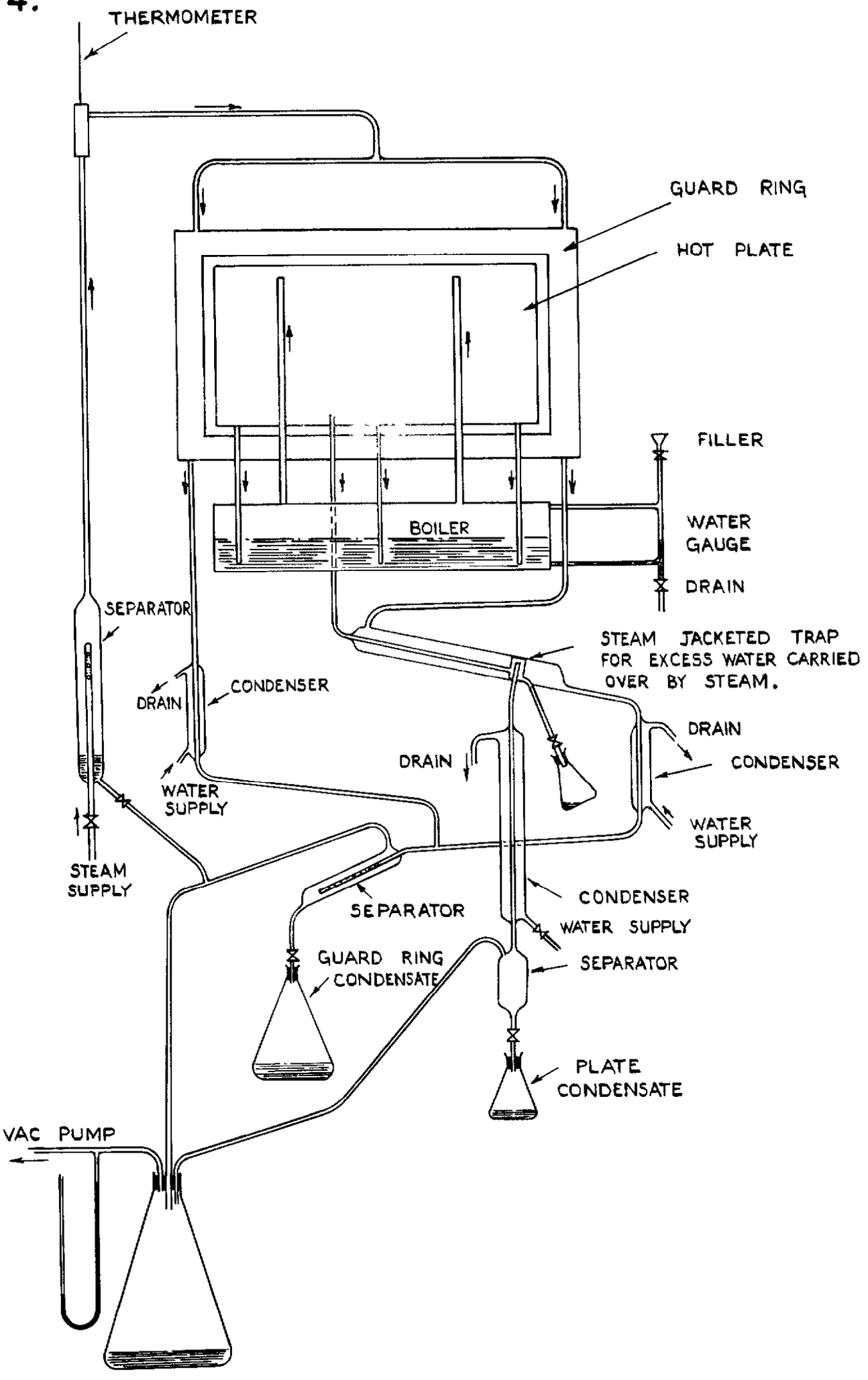

FIG. 4. DIAGRAM OF STEAM AND WATER CONNECTIONS.
(REDUCED PRESSURE)

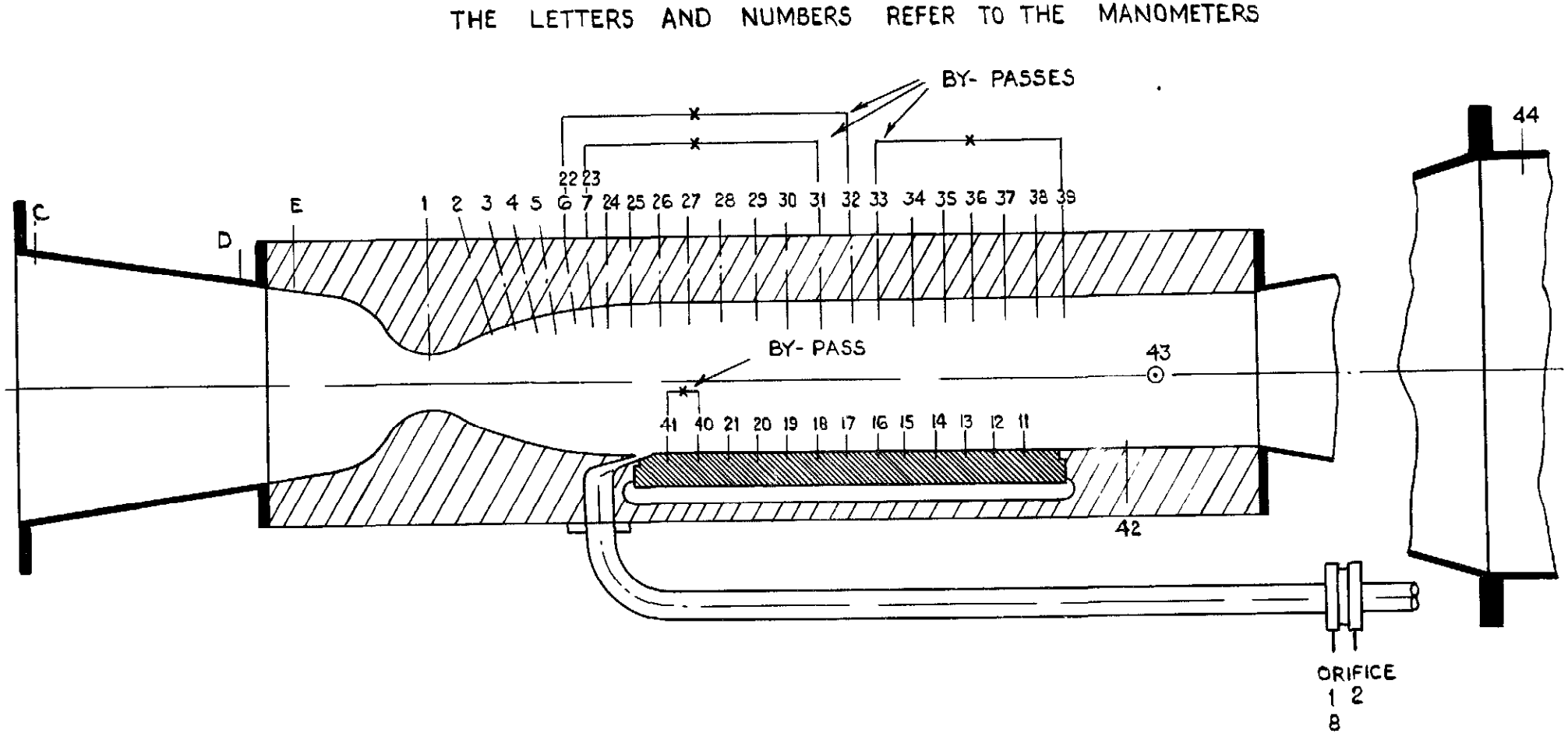

FIG. 5. LOCATION OF STATIC PRESSURE POINTS IN TUNNEL AND HOT PLATE.

FIG.5.

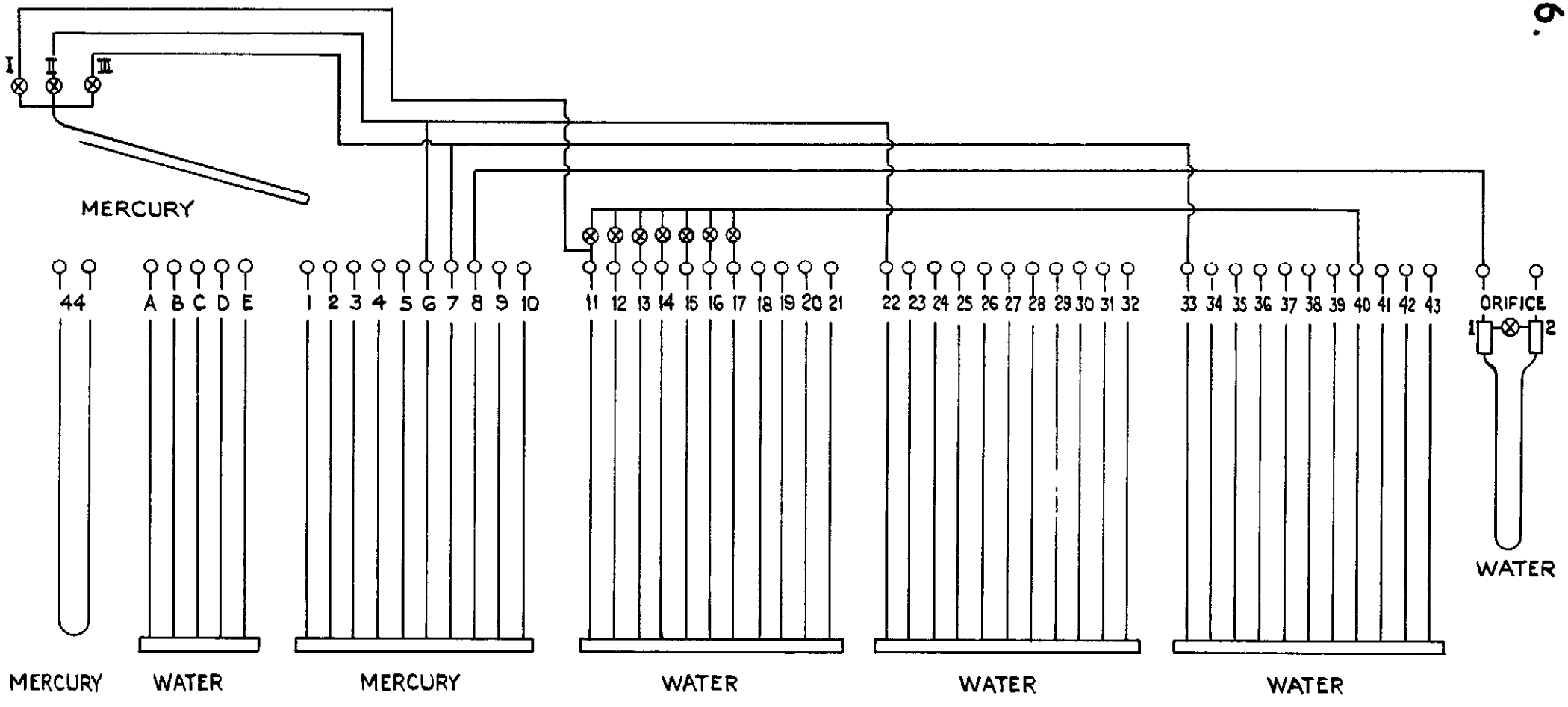

FIG. 6.

FIG. 6. ARRANGEMENT OF MANOMETERS.

FIG. 7.

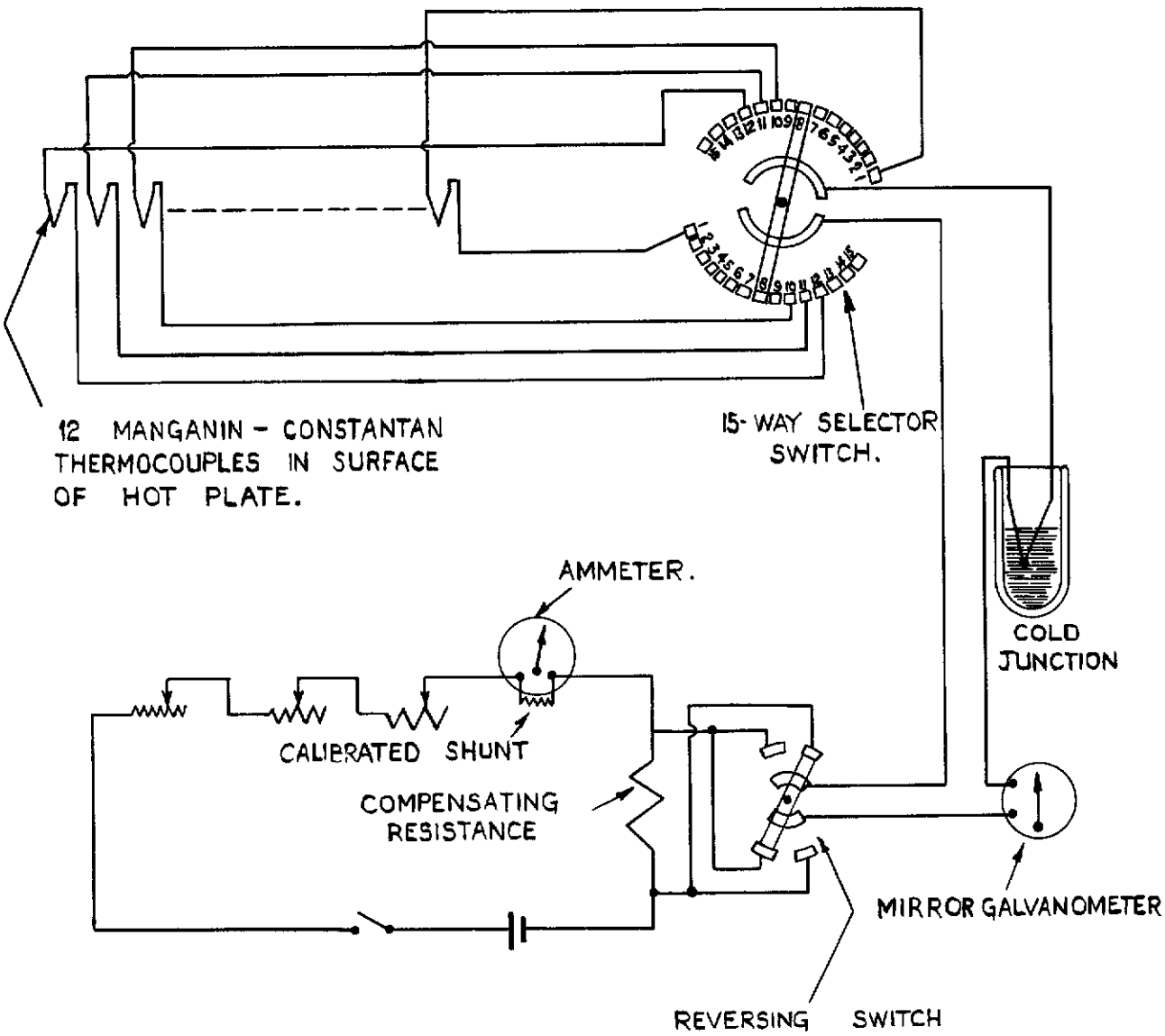

FIG. 7. DIAGRAM OF COMPENSATOR CIRCUIT.

FIG. 8.

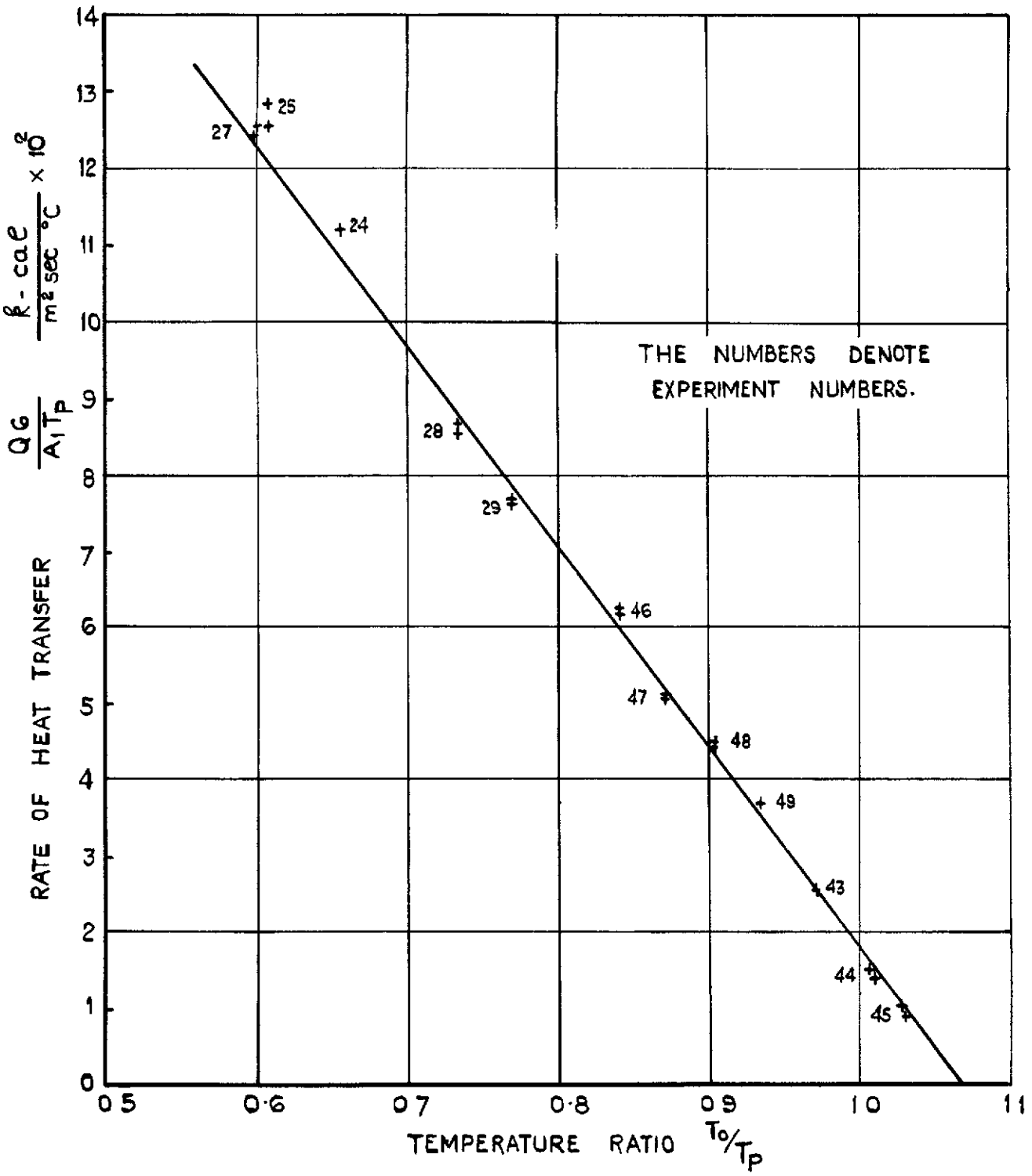

FIG. 8. VARIATION OF HEAT TRANSFER WITH TEMPERATURE RATIO.

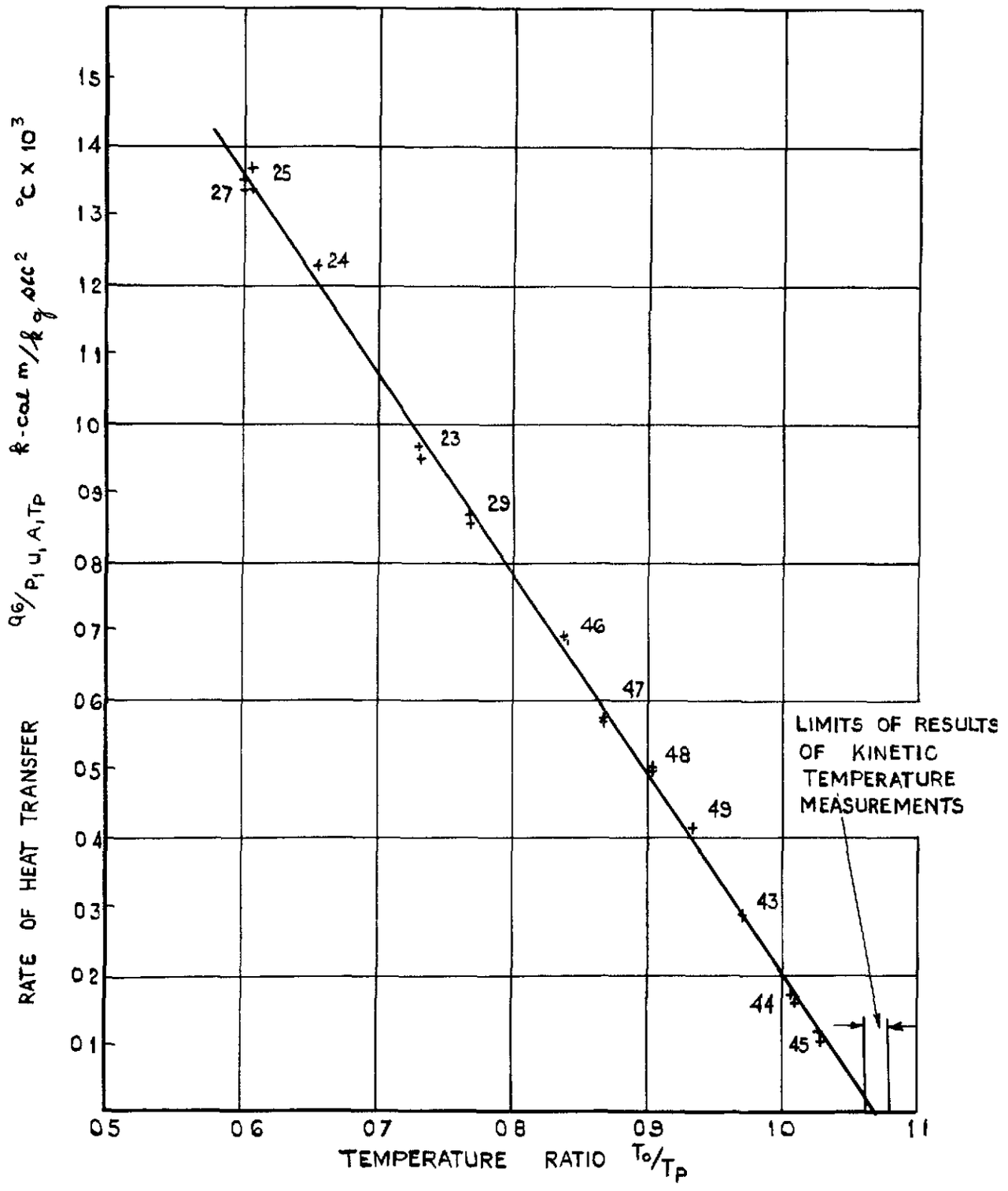

FIG. 9. VARIATION OF HEAT TRANSFER WITH TEMPERATURE RATIO.

EXPERIMENTAL RESULTS FAIRED ONTO A VALUE OF $\frac{u_1}{\sqrt{}} = 10^7$ 1/METRES

FIG.10.

$$\bar{k}_R = \frac{Q_{6/s}}{\rho_1 \mu_1 g C_p (T_p - T_w)}$$

$\bar{k}_R$ = MEAN LOCAL HEAT TRANSFER COEFFICIENT

T_p = HOT PLATE TEMPERATURE

T_w = WALL TEMPERATURE

(ASSUMED EQUAL TO 0 935 T_0, WHERE T_0 IS THE FREE STREAM. STAGNATION TEMPERATURE.)

⊙ EXPERIMENTAL VALUES (σ DENOTES SEVERAL COINCIDENT VALUES)

X, +, Δ CALCULATED VALUES, USING FORMULA

$$\frac{1}{\bar{k}_R} = \frac{\rho_1 \mu_1^2}{\tau_0} + 5\sqrt{\frac{\rho_1 \mu_1^2}{\tau_0}}\left[(\sigma-1) + \ln\left\{1+\tfrac{5}{6}(\sigma-1)\right\}\right]$$

WITH $\sigma = 0.72$, $\frac{\mu_1}{\nu_1} = 2.4 \times 10^5$

X USING BOUNDARY LAYER APPROXIMATION Nº 1

\+ " " " " " 2

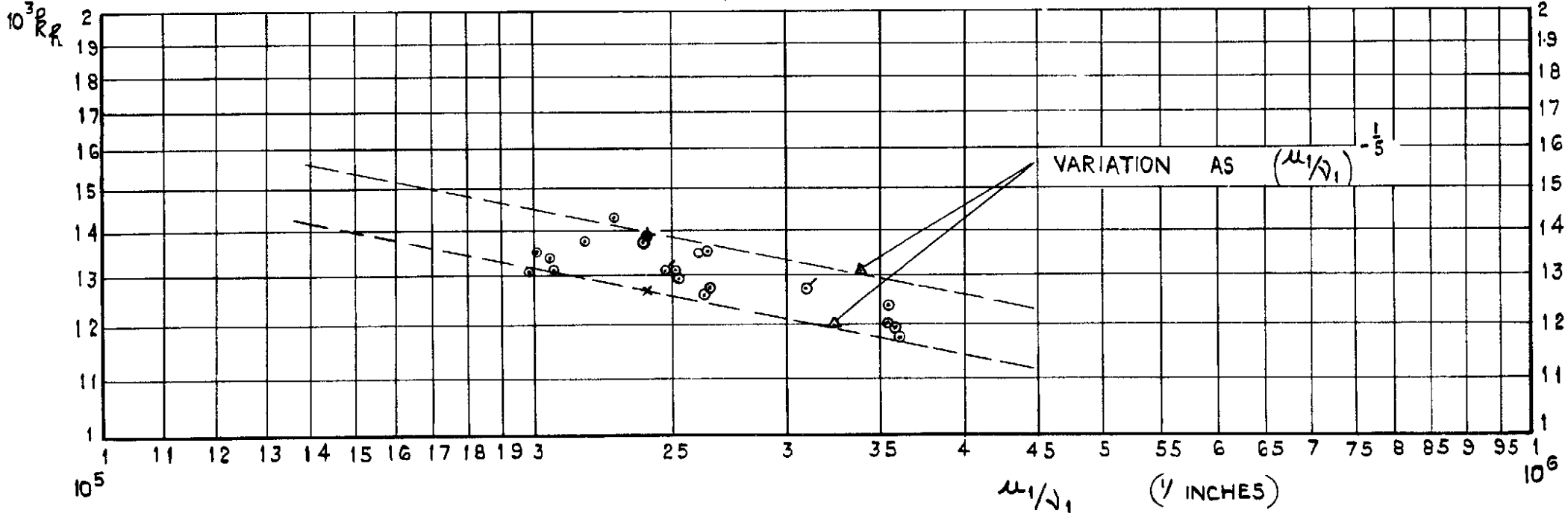

FIG. 10. MEAN HEAT TRANSFER COEFFICIENT $\bar{k}_h$, AT M = 2·5.

FIG. II.

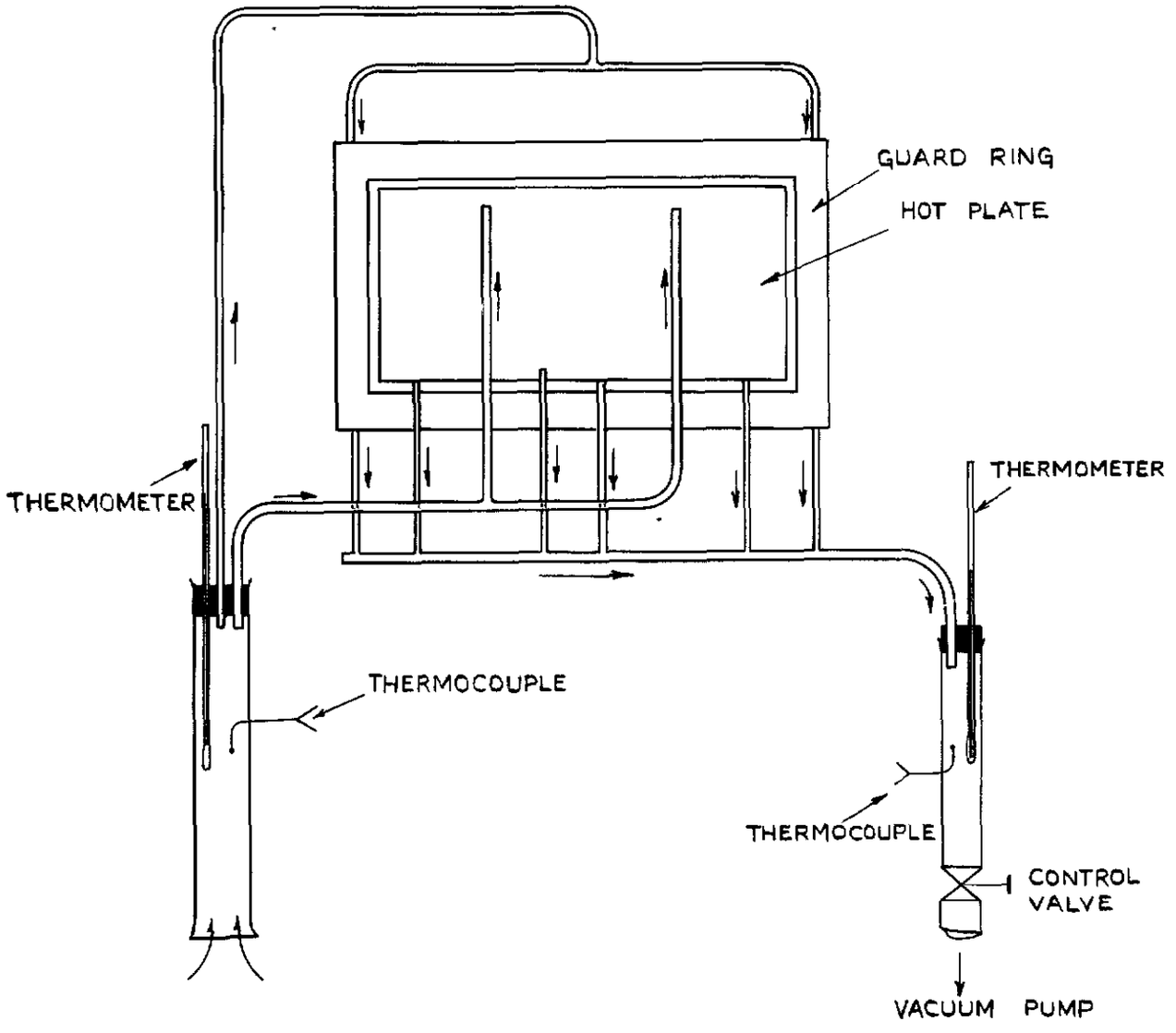

FIG. II. ARRANGEMENT OF HOT PLATE FOR KINETIC TEMPERATURE TESTS.

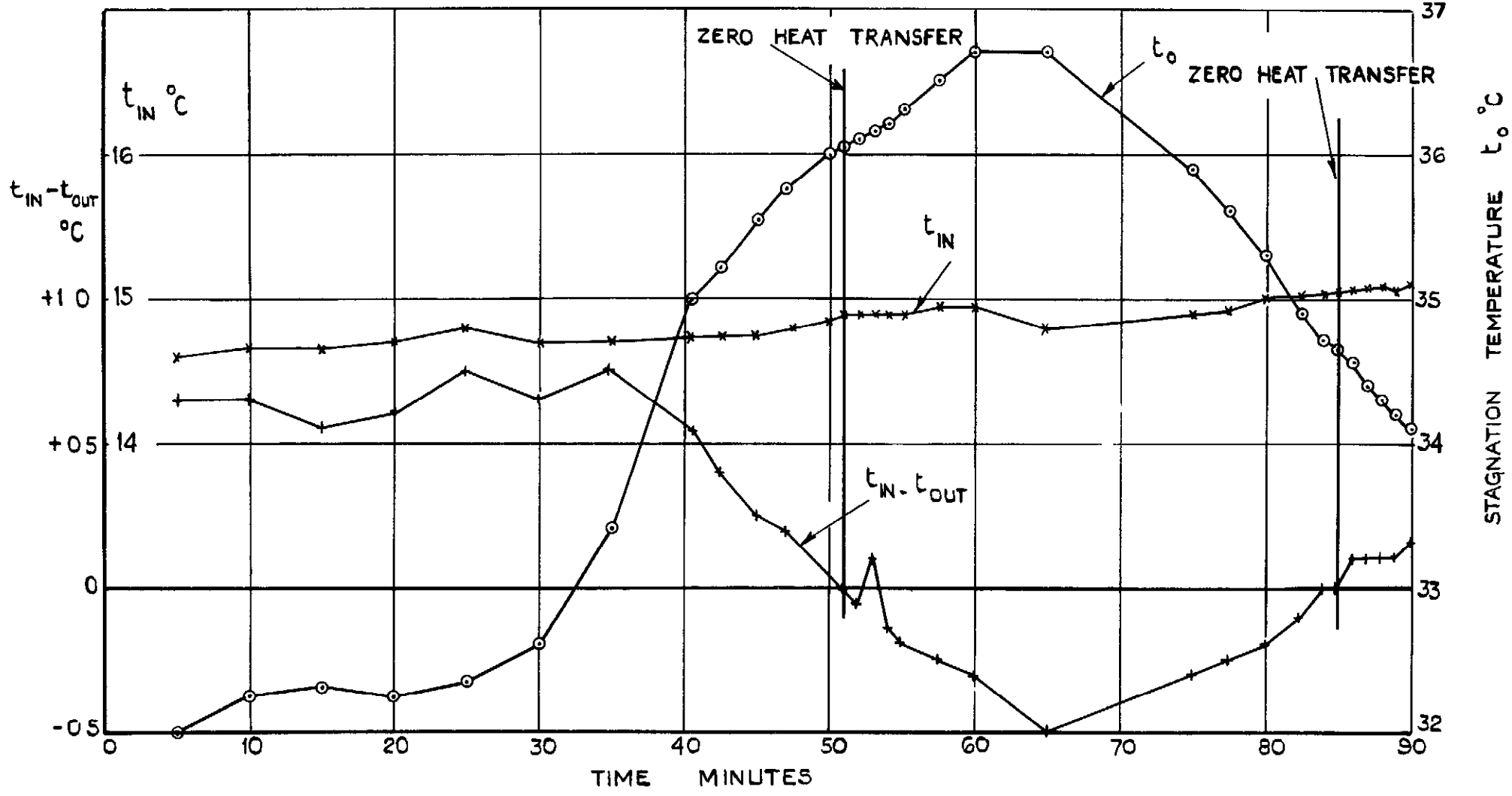

FIG. 12. KINETIC TEMPERATURE MEASUREMENT.

FIG. 12

FIG. 13.

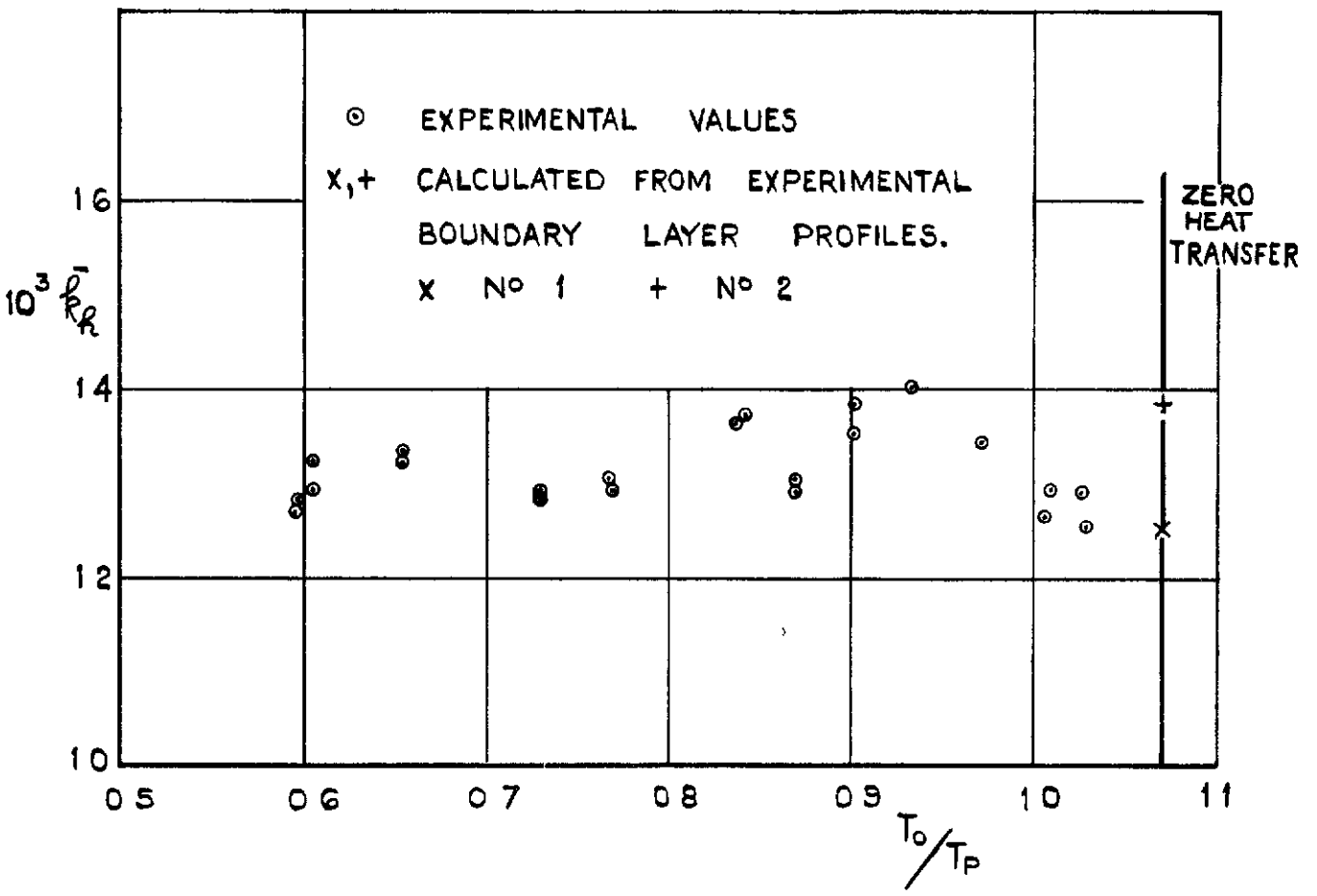

T_o = FREE STREAM STAGNATION TEMPERATURE

T_p = HOT PLATE TEMPERATURE

EXPERIMENTAL $\bar{k}_h$ VALUES ASSUMED TO VARY AS $\left(\frac{\mu_1}{\nu_1}\right)^{-\frac{1}{5}}$

FIG. 13. VARIATION OF $\bar{k}_h$ WITH T_o/T_p FOR $\frac{\mu_1}{\nu_1} = 2{\cdot}54 \times 10^5$ (1/INCHES.)

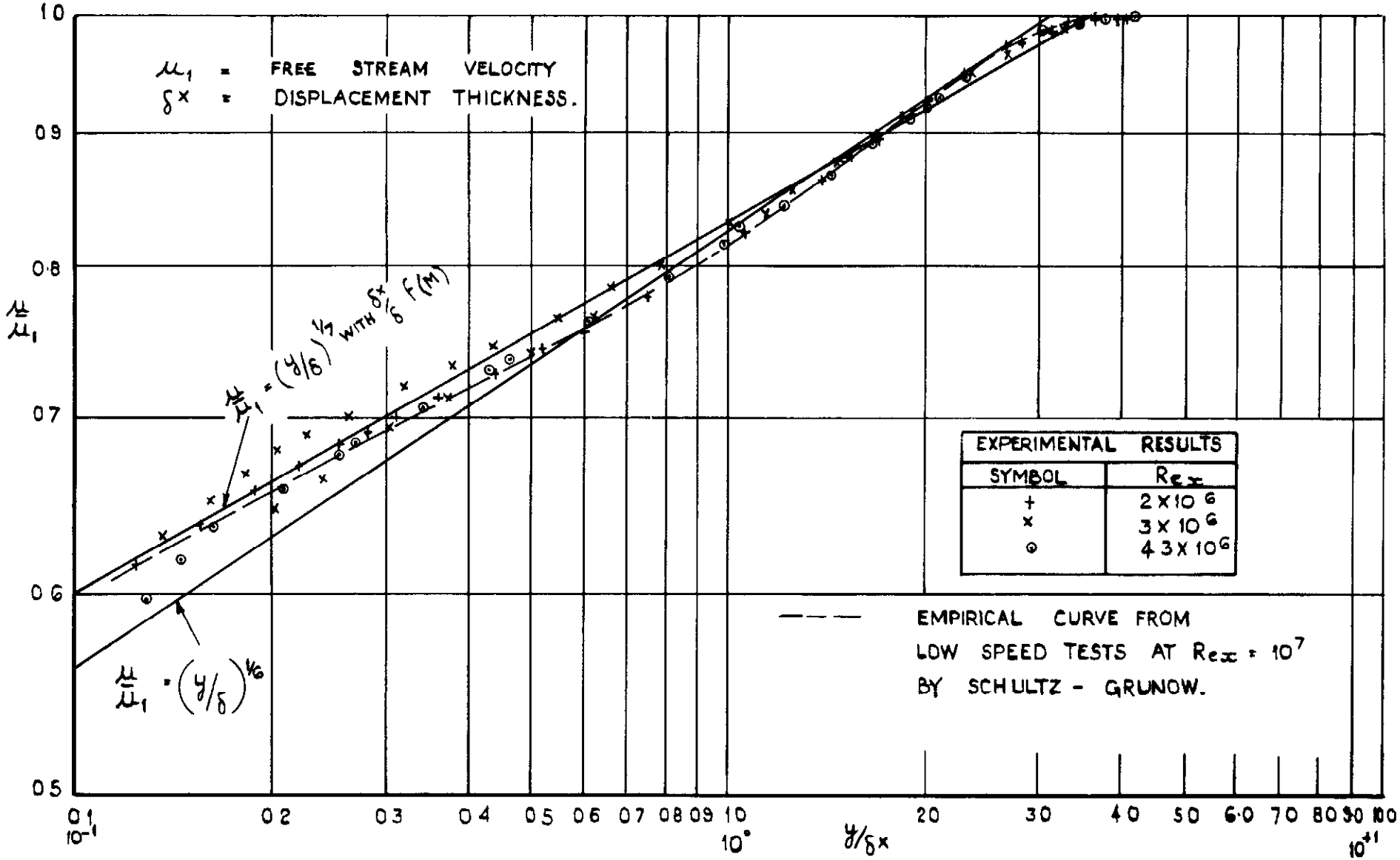

FIG. 14. VELOCITY PROFILES IN BOUNDARY LAYER AT ZERO HEAT TRANSFER CONDITION.

FIG. 14.

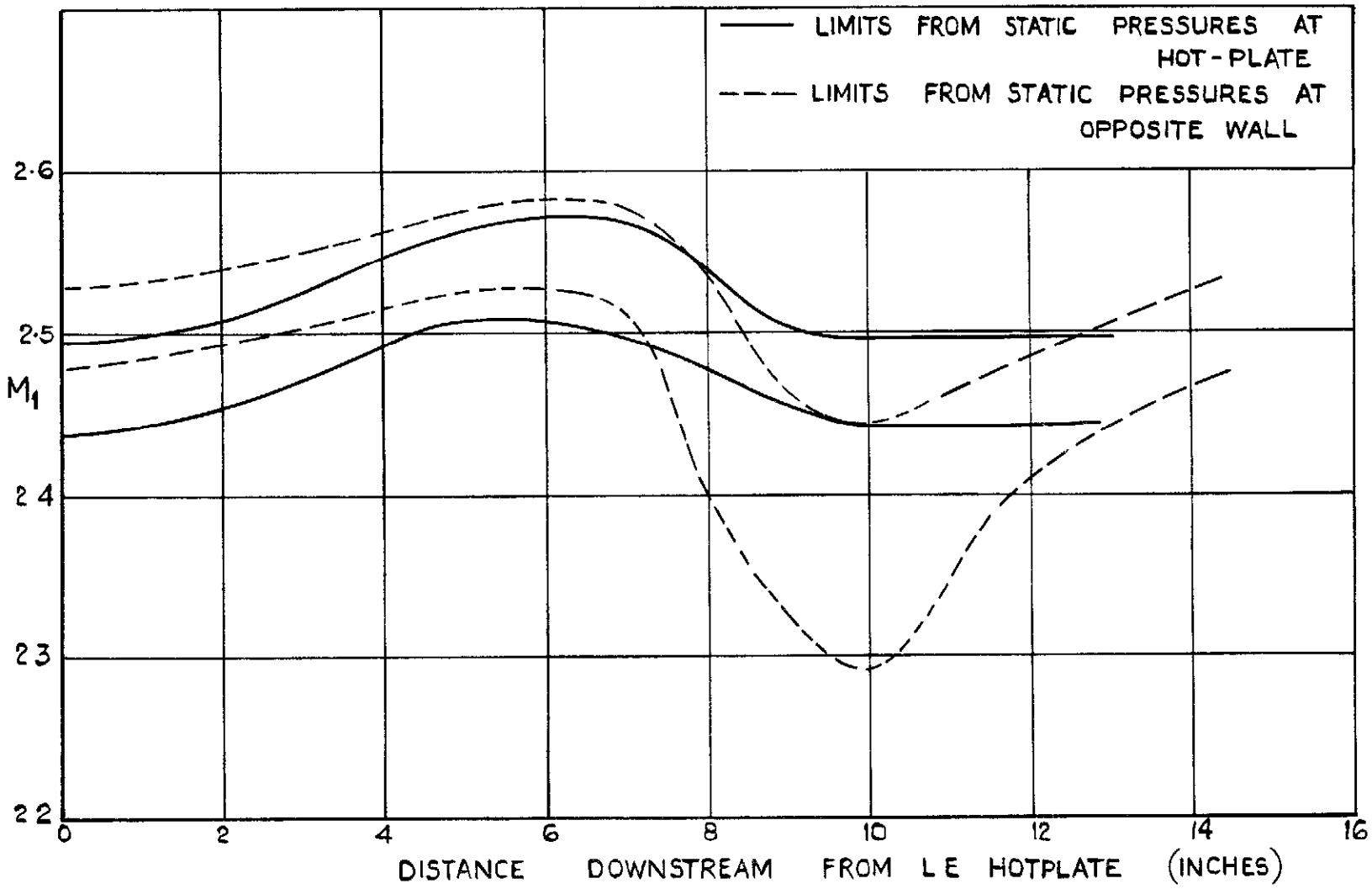

FIG.15. UPPER AND LOWER LIMITS TO FREE STREAM MACH NUMBER. DISTRIBUTION ALONG TUNNEL.

FIG.15.

FIG. 16.

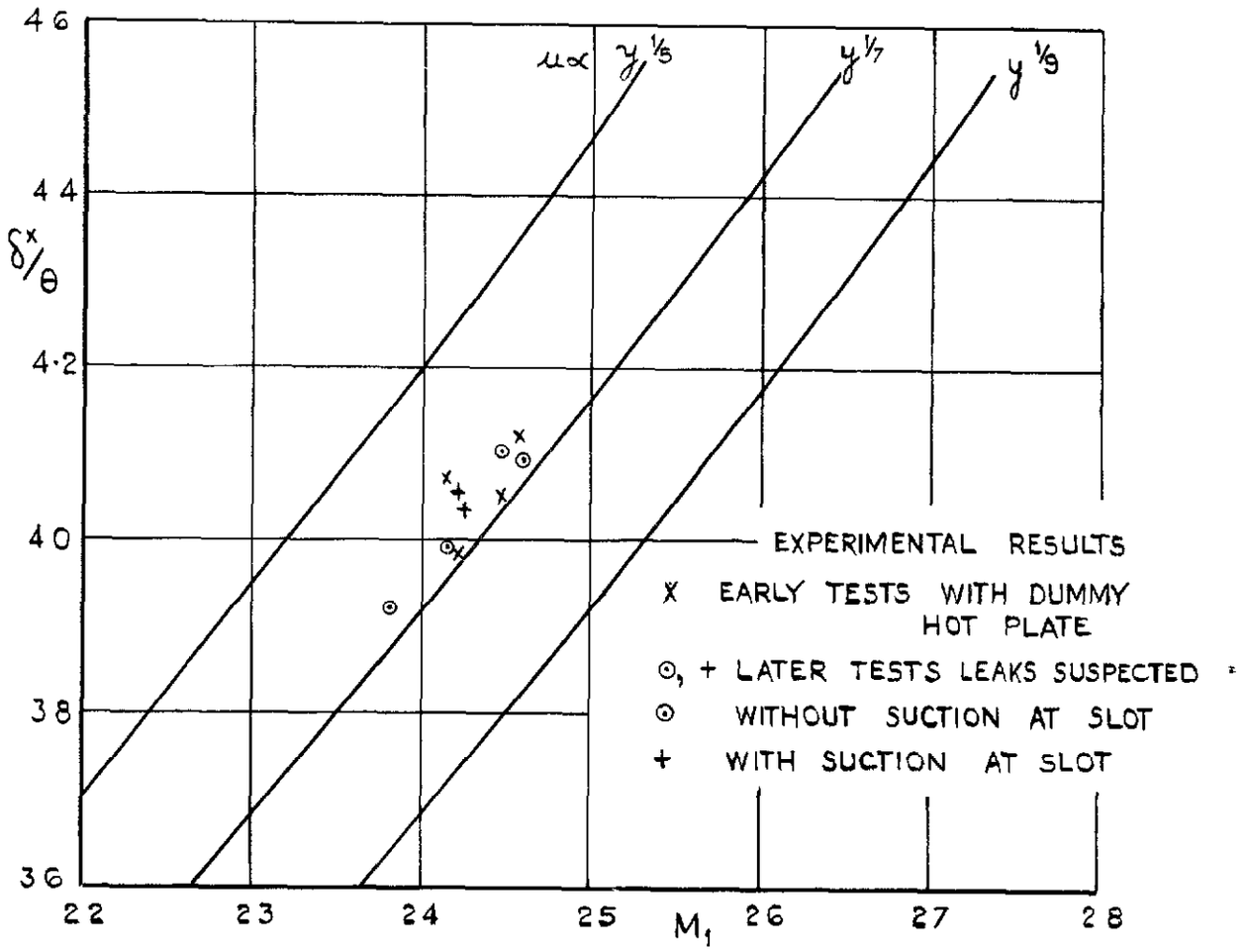

FIG. 16. RATIO OF DISPLACEMENT THICKNESS TO MOMENTUM THICKNESS.
(ZERO HEAT TRANSFER CONDITIONS.)

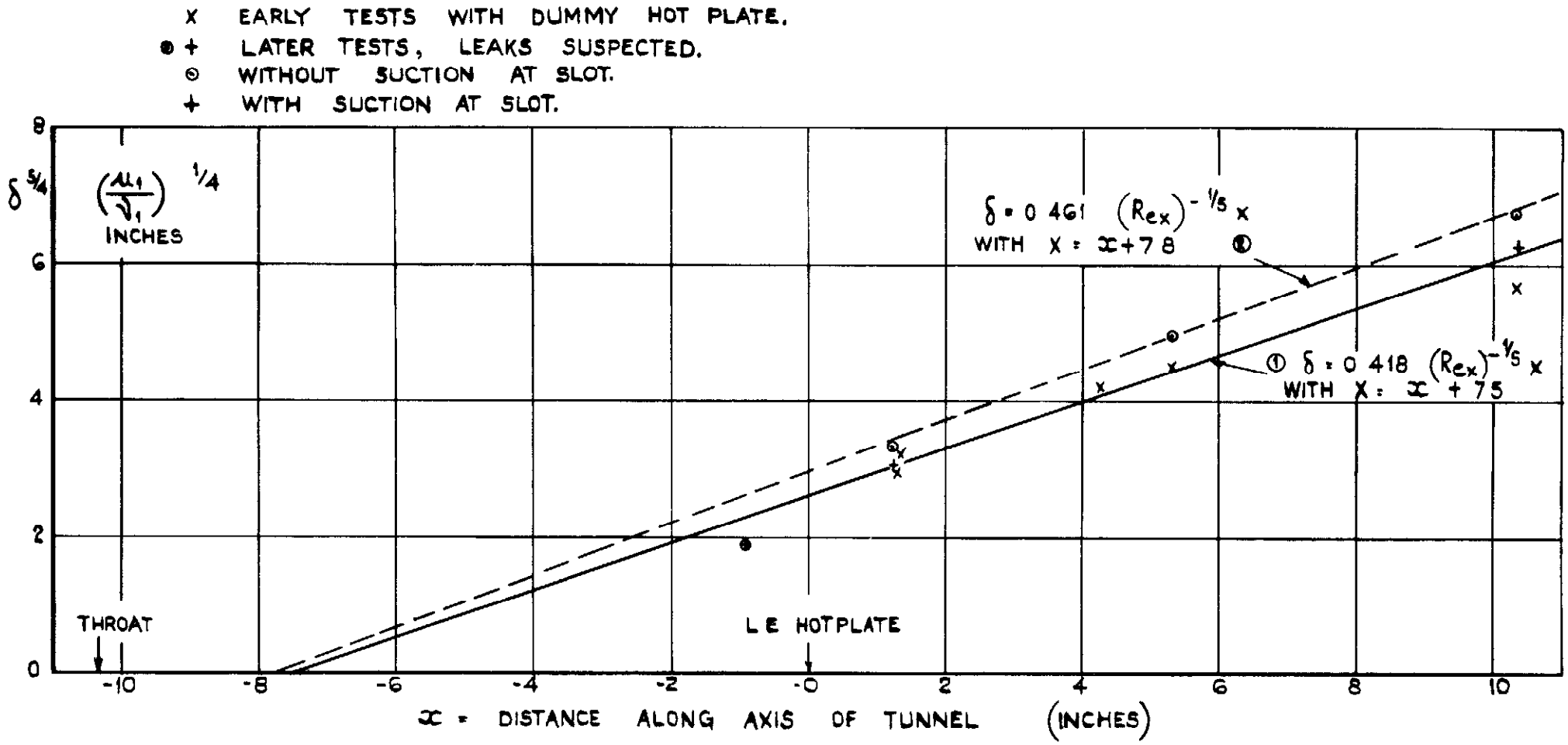

FIG.17. BOUNDARY LAYER THICKNESS IN THE ZERO HEAT TRANSFER CONDITION.
(EXPERIMENTAL VALUES ARE MEAN OF SCALED-UP VALUES OF DISPLACEMENT AND MOMENTUM THICKNESS ACCORDING TO 1/7 POWER LAW. SEE TABLE III.)

FIG. 17

C.P. No. 59
12483
A.R.C. Technical Report

PUBLISHED BY HIS MAJESTY'S STATIONERY OFFICE

To be purchased from :

York House, Kingsway, LONDON, W.C.2, 429 Oxford Street, LONDON, W.1,
P.O. Box 569, LONDON, S.E.1,
13a Castle Street, EDINBURGH, 2. | 1 St. Andrew's Crescent, CARDIFF.
39 King Street, MANCHESTER, 2. | 1 Tower Lane, BRISTOL, 1.
2 Edmund Street, BIRMINGHAM, 3. | 80 Chichester Street, BELFAST,
or from any Bookseller

1951

Price 6s. 0d. net

PRINTED IN GREAT BRITAIN

S.O. Code No. 23-9006-59